



Sprayable engineered cementitious composites (ECC) using calcined clay limestone cement (LC3) and PP fiber

He Zhu, Kequan Yu, Victor C. Li*

Department of Civil and Environmental Engineering, University of Michigan, Ann Arbor, MI, 48109, USA



ARTICLE INFO

Keywords:

Engineered cementitious composites (ECC)
Limestone calcined clay cement (LC3)
Spray
Calcium sulfoaluminate (CSA) additive
PP fiber

ABSTRACT

Sprayable engineered cementitious composites (ECC) has demonstrated in field applications as a promising repair material. However, the large cement dosage that leads to a high carbon footprint and potential restrained shrinkage cracking suggests needed improvements. In this study, a sprayable ECC was developed using calcined clay limestone cement (LC3), calcium sulfoaluminate (CSA) expansive additive and polypropylene (PP) fiber to increase the material greenness and durability. The sprayability and mechanical performance were examined by the flow table and uniaxial tension tests. The one-time build-up thickness achieved was 45 mm for vertical spraying and 35 mm for overhead spraying at 20–30 min rest-time, and up to 80 mm for vertical spraying at 50 min rest-time. The ECC had a comparable strength but higher tensile strain capacity (5.7%) and reduced crack width (30 µm at 1% tensile strain) when sprayed, in comparison to specimens prepared by casting. A spray-repaired layered ECC-concrete composite revealed multiple cracking and strain-hardening performance under flexural loading. The advantages of low carbon, low shrinkage, low cost, and ultra-high ductility of the developed sprayable ECC promote broader applications in infrastructure repair.

1. Introduction

Concrete is the most widely used construction material due to its good mechanical performance, longevity, low cost, and wide availability [1,2]. However, due to its brittleness, concrete suffers from cracking that lowers the safety and durability of structures. Shotcrete technology is attractive for infrastructure repair with advantages of mold-free, cost-effectiveness, less variation in mechanical performance, and high construction efficiency but remains quasi-brittle even when reinforced with steel fibers [3].

Engineered Cementitious Composites (ECC) is a fiber-reinforced ductile concrete designed for at least a 3% tensile strain capacity [1]. Sprayable ECC [4,5] has been developed with rheology controlled by water reducer, viscosity modified agent, and calcium aluminate (CA) cement. Structures repaired or retrofitted with sprayable ECC include irrigation channels [6], tunnel lining [6], masonry walls [7], dams [8,9], and culverts [10]. However, the high cement dosage in ECC compositions increases the environmental concerns of CO₂ emissions, since 5–8% of the total anthropogenic CO₂ emissions are attributed to cement production [1,11]. Additionally, the large cement volume of ECC results in considerable shrinkage up to 1500 µε at 28 days [12,13], increasing

the restrained cracking risk [14,15]. Therefore, sprayable ECC can be further enhanced in both environmental and shrinkage-reduction aspects.

In recent years, calcined clay limestone cement (LC3) has been developed for mitigating the environmental impacts of cement production [16,17]. The LC3 cement incorporating 50% clinker, 30% calcined clay, 15% limestone, and 5% gypsum reduces 20–35% of CO₂ emissions compared with ordinary Portland cement (OPC) [11,18]. In one study [19], the introduction of LC3 into ECC composition provides a 48% reduction of carbon emission compared to conventional M45-ECC. Meanwhile, the novel LC3-ECC exhibited a tensile strain capacity larger than 6% and good durability due to the tight crack width. A medium-strength ECC with 33–65 MPa of compressive strength at 28 d was developed based on LC3 cement; however, the tensile strain capacity was reduced to 0.57–1.58% [20]. LC3 has shown viability in developing low carbon ECC with superior tensile ductility but has not been used in spray applications. The altered rheology of LC3 paste [21,22] is expected to influence the pumpability and sprayability of LC3 cement. There is a need to investigate the rheological property of LC3-based ECC for spray applications.

The expansive calcium sulfoaluminate (CSA) cement/additive

* Corresponding author.

E-mail addresses: zhuhe14@tsinghua.org.cn (H. Zhu), kequany@umich.edu (K. Yu), vcli@umich.edu (V.C. Li).

possesses the advantages of shrinkage compensation and rapid hardening, suggesting its advantageous incorporation in sprayable ECC. By increasing the CSA content, low shrinkage or expansion could be obtained [23,24]. On the other hand, the CSA has a significant effect on rheology development due to the rapid hardening property [25]. Rapid hardening CA cement, similar to CSA, was utilized for sprayable ECC [4], in which 5% of CA replacement of OPC obtained two-stage rheology suitable for spraying [4]. However, excessive CA (10%) resulted in a rapid increase of viscosity adverse to spray application. It is hypothesized that a low shrinkage CSA-containing ECC may be developed for spraying by adopting a moderate CSA ratio; however, its flowability and sprayability require deliberate design and careful examination.

ECC usually employs a 2% by volume of synthetic fiber. Polyvinyl Alcohol (PVA) fiber [4,8], polyethylene (PE) fiber [26–28], and high-tenacity polypropylene (HTPP) fiber [19,29,30] are the most commonly used fibers. Despite the disadvantage of lower strength and stiffness, PP fiber shows promise as a lower-cost fiber than PVA or PE in ECC designed for repair applications. Due to the smaller diameter, the number of PP fiber (12 µm diameter) is about 10.6 times of PVA fiber (39 µm diameter) for a given dosage and the same fiber length [30]. The enlarged quantity of PP fiber increases the difficulty of ECC pumpability and sprayability. The matrix rheology also affects the PP fiber dispersion and mechanical performance of hardened PP-ECC [31]. 1.5% PP fiber is utilized to develop a sprayable ECC [29]; however, the mechanical performance (0.87 MPa ultimate tensile strength and 1% tensile strain capacity at 28 days) is inadequate for structural repair. To develop a sprayable PP-ECC for structural repair with at least 2.5 MPa ultimate tensile strength and 3% tensile strain capacity, a larger fiber dosage (at least 2% volume fraction) is needed, which requires rheology control of the LC3 matrix to assure suitable pumpability and sprayability.

This research aims at developing a sprayable ECC with advantages of ultra-high ductility, low-shrinkage, low-carbon, and low-cost. LC3 cement, CSA additive, and 2% volume of PP fiber were utilized to attain these objectives. The flowability range suitable for spraying was evaluated by flow table test conforming to ASTM C1437 [32]. Spray tests were conducted to verify the sprayability and sprayed layer build-up ability. The mechanical properties of the sprayed ECC were investigated in terms of compressive strength, tensile performance, flexural performance, and interfacial bonding strength between ECC and concrete.

2. Design of sprayable ECC

Control of fresh property is crucial for ECC processing to obtain different types of ECC. Cast, sprayable, self-consolidating, and extruded ECC has been developed by adjusting the rheology of the fresh matrix [1]. While different indices such as viscosity, tribology, and pump

pressure [4,33,34] have been used for shotcrete design, the deformability obtained by a mini-slump flow test is proposed here as a simple and practical index for characterizing the rheology properties [35]. Fig. 1 depicts the conceptual design principle of sprayable ECC using the deformability index (defined in Section 3.2). The requirements of rheology control vary with different processing stages as follows:

- (1) **Mixing stage:** A moderate viscosity assures the fiber dispersion uniformity, leading to a robust strain-hardening property [31]. Furthermore, lower flowability is preferred for PP-ECC to attain a robust strain-hardening effect [30].
- (2) **Pumping stage:** Before spraying, the fresh ECC is conveyed from the mixer to the spraying nozzle by a pump. To pump through the hose under proper pump pressure, the fresh ECC requires adequate initial high deformability, defined as the minimum pumping deformability (D_{min}^{pump}) in Fig. 1. Since workability experiences reduction during the time interval between the end of mixing and start of pumping, the D_{min}^{pump} is smaller than the minimum deformability of robust ductility. On the other hand, a high flowable matrix, even like water, can be pumped, but the low viscosity is inadequate for dispersing the PP fiber. Hence, the range of deformability index for pumpability is larger than that for robust ductility.
- (3) **Spraying stage:** Spray quality is determined by many factors, such as spray gun pattern, nozzle skill, spray direction, air pressure, and material cohesion. Material cohesion is one of the most critical factors to determine the atomization ability at the nozzle of the sprayed ECC. The minimum required deformability for atomization is named D_{min}^{spray} in Fig. 1.
- (4) **Build-up stage:** A two-stage rheological property was designed for sprayable ECC [4]. During the first stage (before spraying), high deformability is desired for mixing, pumping, and accommodation of required work-time. In the second stage (after spraying), the deformability of fresh ECC should decrease rapidly to allow the building-up of enough thickness of the repair material on the substrate. Rest time is defined as the time just after mixing and before spraying. Optimal rest time is required according to the above two-stage rheological property to obtain a good atomization quality and build-up ability. The maximum allowable deformability for building up required thickness is defined as D_{max}^{spray} .

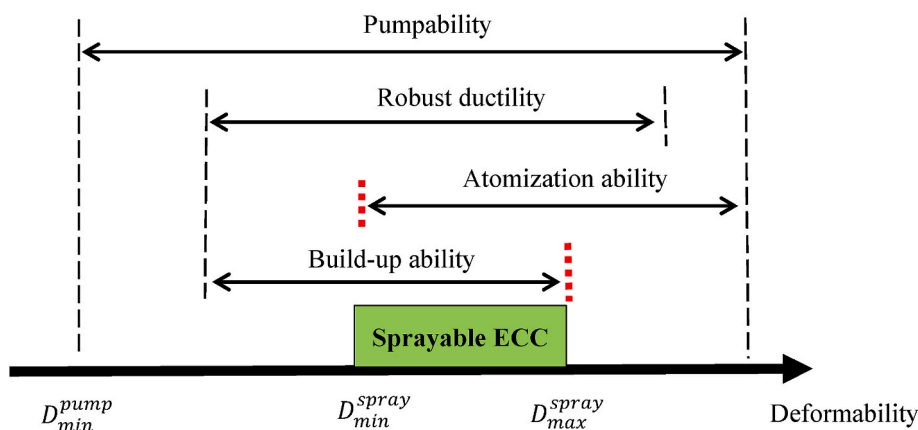


Fig. 1. The material deformability principle for designing the sprayable ECC. Sprayable ECC is designed to achieve a deformation index $D_{min}^{spray} < D < D_{max}^{spray}$ to meet requirements for pumpability, robust ductility, atomization ability, and build-up ability.

3. Experimental program

3.1. Materials

The mixture in this study was developed according to Ref. [19], where the composite cement comprised 63 kg/m³ of OPC (Type I, Lafarge Holcim Cement Co), 147 kg/m³ of metakaolin (MK, Sikacrete® M – 100), 73 kg/m³ of limestone (LS, Omya), and 206 kg/m³ of CSA. The CSA weight was proposed by the manufacturer (Komponent®, CTS Cement Manufacturing Corp) to obtain a shrinkage compensation effect. 1077 kg/m³ of fly ash (FA, Boral Material Technologies Inc) was used to increase the greenness of the ECC composition. The 12 µm diameter and 10 mm length PP fiber (Saint-Gobain Brazil) has 6 GPa Young's modulus and 850 MPa tensile strength. The PP content was 2% by volume, while the water/binder ratio was 0.3. Water reducer (WR, AVDA® 190 from GCP Applied Technologies) was incorporated at 0.7%, 0.8%, and 0.9% weight of the binder. The mix proportions are listed in Table 1.

3.2. Spray test

A mini-slump cone (diameter $d_0 = 10$ cm) was used for measuring and quantifying the deformability. During sample preparation, all solid ingredients were mixed in a 5.6-liter mixer for 10 min. The water pre-mixed with SP was then added to the dry ingredients and mixed for 6 min at 100 rpm. Finally, 2% of PP fibers were added and mixed at 200 rpm for an additional 6 min. The resulting fresh ECC was used for the flow table test at 10-min intervals. After lifting the inverted cone away from the ECC, the table was dropped 25 times in 15 s according to ASTM C1437 [32]. The maximum spread diameter (d_1) and the diameter perpendicular to d_1 (marked as d_2) were recorded and used for calculating the deformability index (D) [4] as follows:

$$D = \frac{(d_1 \times d_2) - d_0^2}{d_0^2} \quad (1)$$

For developing a new sprayable ECC, the optimization of flowability suitable for spraying requires trial tests. For this purpose, and for reducing the required materials, labor, and time necessary for a full-scale spray test, a hand-held 3.5-liter spray hopper was utilized to investigate the relationships of rest time, WR content, and maximum build-up thickness. As shown in Fig. 2, the air inlet was connected with a 500 kPa air system, and the ECC was sprayed out from the 8 mm diameter nozzle onto a vertical plywood substrate. The spray tests were performed every 5 min and lasted 2 min. After each test, the maximum build-up thickness was recorded. The video recording the process of spray tests can be found in the Appendix.

After obtaining the target flowability by the small spray hopper, spray tests with a larger volume of ECC were conducted using a CARROUSEL® pump on wheels (Fig. 3) available from Quikspray® to demonstrate robust sprayability. 30-liter ECC was mixed by a Hobart mixer following the same procedure as the flow table test (sequence of dry material-fluid-fiber mixing). After 20 min rest-time, the ECC was sprayed onto a vertical and overhead plywood substrate using 500 kPa air pressure.

3.3. Mechanical performance test

The samples of ECC were prepared by both cast and sprayed methods, where the cast samples were vibrated for 30 s. No vibration

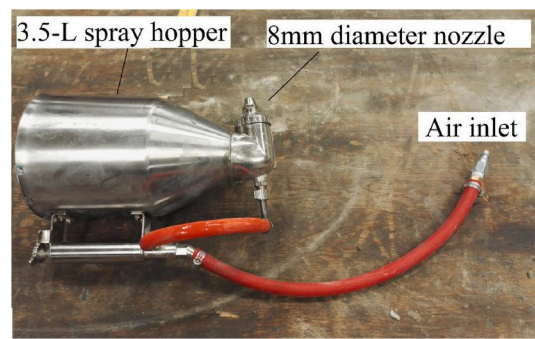


Fig. 2. The spray hopper for build-up thickness tests.

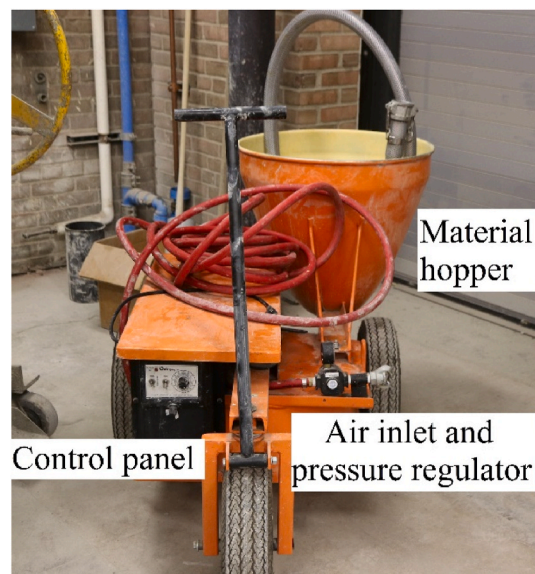


Fig. 3. The CARROUSEL® pump from Quikspray® for spray test with 30-liter ECC.

was applied to the sprayed samples. Only the ECC with 0.8% solid weight of WR was used in the mechanical performance test due to their preferred rheological properties (Section 4.1). To prepare the 50 mm cubes and dogbone specimens, their molds were placed on the ground, and the ECC was sprayed directly or cast into the molds (Fig. 4). The excess materials outside the dogbone molds (Fig. 4) were removed once the spraying was finished. The rough surface was trowelled along one-direction gently and carefully at the rest-time of 40 min when the ECC had the build-up ability so that the surface finishing process had minimum effect on the internal porosity and fiber alignment, which differed from the cast samples. It should be noted that surface trowelling is always adopted in practical engineering, and may improve the density and fiber alignment of the sprayed ECC, particular those with thinner thickness [36].

The specimens were demolded 24 h later. After curing for 28 days in 20 ± 3 °C and 40 ± 5% RH environment, the cube samples were tested under compression loading according to ASTM C109 [37]. The dogbone specimens were tested on an Instron system at a rate of 0.5 mm/min. Two linear variable displacement transducers (LVDT) with an 80 mm gauge length were employed to measure the deformation [19]. The average and maximum crack width were measured per [19,30], respectively.

The interfacial bond strength and bending behavior between the concrete substrate and ECC were studied. The concrete [5] used natural river sand (particle size of 0.3–4 mm and a sand/binder ratio of 1.62),

Table 1
Mix ratios of ECC matrix (kg/m³).

Mixture	OPC	CSA	MK	LS	FA	Water	WR
WR-0.7%	63	206	147	73	1077	470	11.0
WR-0.8%	63	206	147	73	1077	470	12.5
WR-0.9%	63	206	147	73	1077	470	14.1

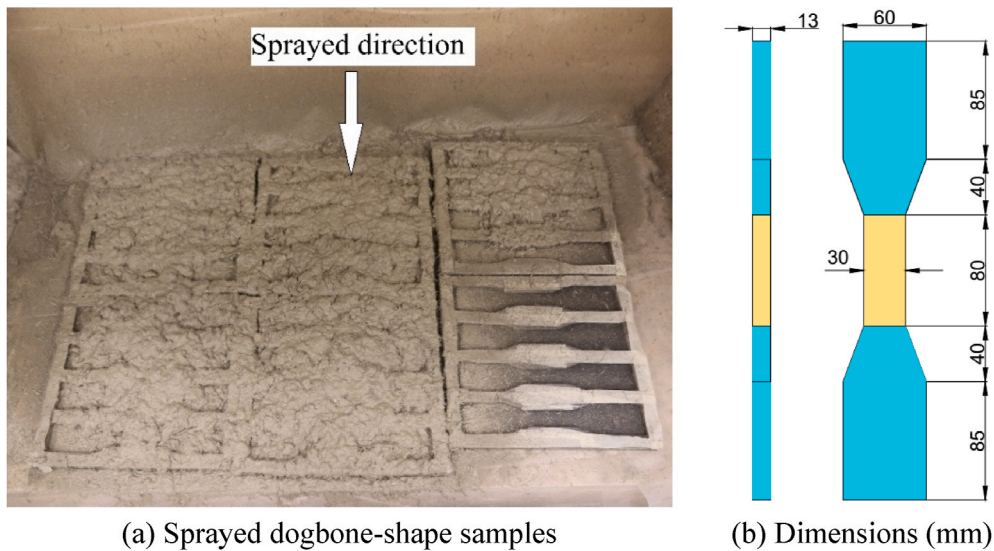


Fig. 4. Dimensions of dogbone-shape mold for uniaxial tension test.

and crushed natural stone coarse aggregate (maximum particle size of 10 mm with weight equal to sand). The water/OPC ratio was 0.45. The concrete was cast into the cube mold (Fig. 5 (a)) and the bending specimen mold (Fig. 6 (a)) to half height. After curing for 28 days, the specimen surface was cleaned with 700 kPa compressed air and then moistened with water. Any excess water on the surface was removed by a paper towel. The rest of the molds was then filled with the cast or sprayed ECC and air-cured for 28 days.

Splitting tensile strength tests (Fig. 5(b)) were conducted on the ECC-concrete composite cubes [8] at a rate of 15 kN/min. As proposed by Ref. [39], the ratio of loading strip width to specimen length (Fig. 5(b)) is designed as 1/6 to minimize the effect of specimen size difference on the measured splitting tensile strength. A correction to the standard formula [38] has been made to account for the non-uniform tensile stress distribution. The corresponding splitting tensile strength is calculated using Eq. (2) [39].

$$f_{split} = 0.61 \frac{P}{A} \quad (2)$$

where P is the applied load of splitting tensile test, and A is the section area of the cube specimens ($100 \times 100 \text{ mm}^2$).

Four-point bending tests (Fig. 6(b)) of layered ECC/Concrete specimens were conducted at a rate of 0.5 mm/min [5], with the ECC positioned on the tensioned side of the beam. The deflection of the bending specimen was measured by two LVDTs attached at the midspan of the

specimen.

4. Results and discussions

4.1. Sprayability

The build-up ability of the sprayed ECC was examined with a small spray hopper (Fig. 2). Fig. 7 depicts the maximum build-up thickness of the sprayed ECC on vertical plywood at different rest-time. The thicknesses of WR-0.8% at the rest times of 10 min, 25 min, and 40 min are shown in Fig. 8. The maximum build-up characteristic showed a two-stage development, consistent with the rheological property described in Ref. [4]. At the early stage, the material was too flowable for building-up on the plywood. There was a distinct turning point in rest-time, however, after which the build-up ability increased significantly due to the rapid hardening of CSA cement.

The rest time of the turning point was approximate 10 min, 18 min, and 30 min for WR-0.7%, WR-0.8%, and WR-0.9%. Before spraying, time is required for the ECC to be pumped and conveyed through the hose to the nozzle. Hence, appropriate rest time should be reserved to meet the expected deformability loss before spraying. The optimal rest time could be larger than 15 min [1] for working and transporting, indicating that the rest time of WR-0.7 is inadequate. Besides, lower flowability is beneficial for the ductility of PP-ECC; therefore, the WR-0.8% was adopted in this study for testing the mechanical performance of the sprayed ECC.

Fig. 9 plots the deformability as a function of rest time for the three mixes with varying amounts of WR. As expected, the deformability decreased with the rest time, while higher WR content resulted in higher initial deformability. The deformability of WR-0.7% was 2.5 at 10 min, equal to that of WR-0.8% at 20 min. The results in Fig. 7 showed that the turning point time of WR-0.7% and WR-0.8% for build-up thickness were around 10 min and 20 min, respectively, indicating that 2.5 was the maximum allowable deformability for the build-up requirement of the sprayable ECC. Though the deformability (>2.5) may build-up enough thickness by increasing the material adhesion such as bonding agent [29] or the surface roughness [8], it is proposed that deformability of 2.5 be conservatively adopted as a maximum value for building-up of sprayed material without sliding off under gravity.

On the other hand, excessively low deformability may hinder ECC sprayability. Below a minimum critical deformability D_{min}^{spray} , the sprayed ECC cannot obtain a good atomization quality. Larger air pressure makes the material easier for atomization. However, the excess pressure causes

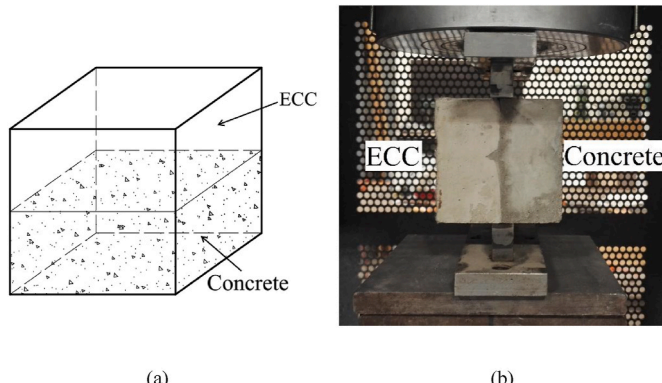


Fig. 5. (a) 100 mm cube specimen and (b) setup of the interfacial split tensile test [8].

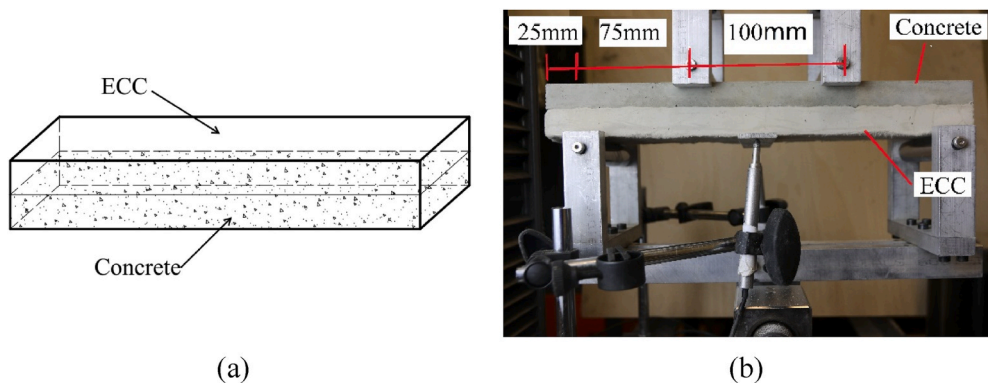


Fig. 6. (a) Bending specimen ($300 \times 76.2 \times 40$ mm) and (b) 4-pt bend test setup.

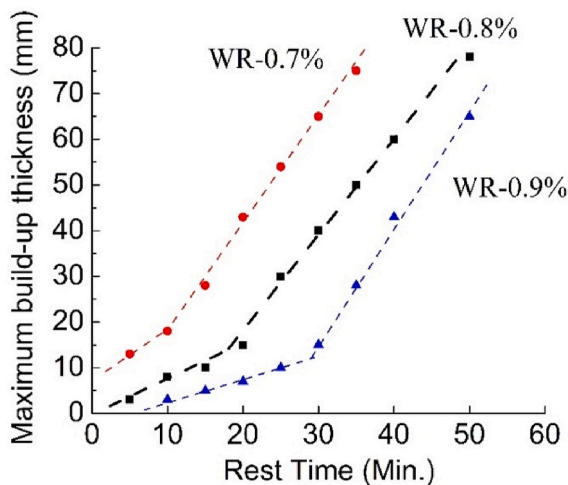


Fig. 7. The relationship of the maximum build-up thickness and rest-time for mixes with different WR levels.

the segregation of PP fiber from the matrix. For the sprayable PP-ECC, PP fibers were found separated from the matrix when the air pressure was larger than 500 kPa. PVA-ECC could tolerate a higher (700 kPa) air pressure without fiber separation because the hydrophilic PVA fiber has a better bonding with the matrix than the hydrophobic PP fiber. The ECC employs fiber for attaining the unique characteristic of multiple cracks and high ductility, which may be lost due to the loss of fiber during the spray process. Thus, the air pressure for spraying PP-ECC was limited to

500 kPa, and $D_{min}^{spray} = 1.8$ was proposed to assure a good atomization quality for sprayable PP-ECC.

Consistent with the results of small spray hopper, the ECC (WR-0.9%) sprayed with CAROUSEL® pump was too flowable for building up thickness at rest time 20 min, while the atomization quality of ECC (WR-0.7%) was unsuitable for spraying after 35 min. Using the proposed deformability range of 1.8–2.5, 30-liter ECC (WR-0.8%) sprayed with the CAROUSEL® pump at rest time 20 min simultaneously meets the

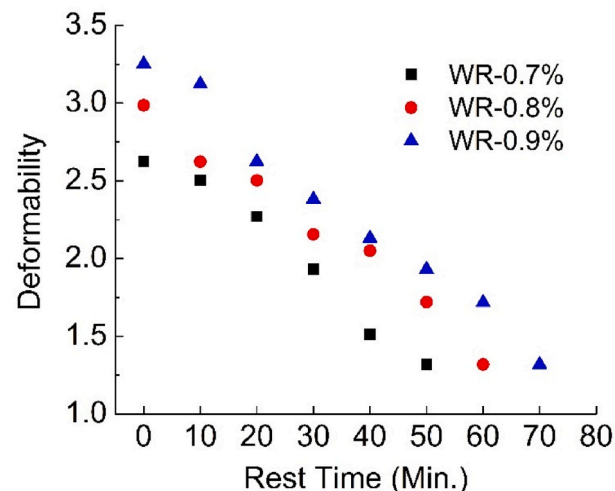


Fig. 9. The decrease in deformability of the sprayed ECC with rest-time.

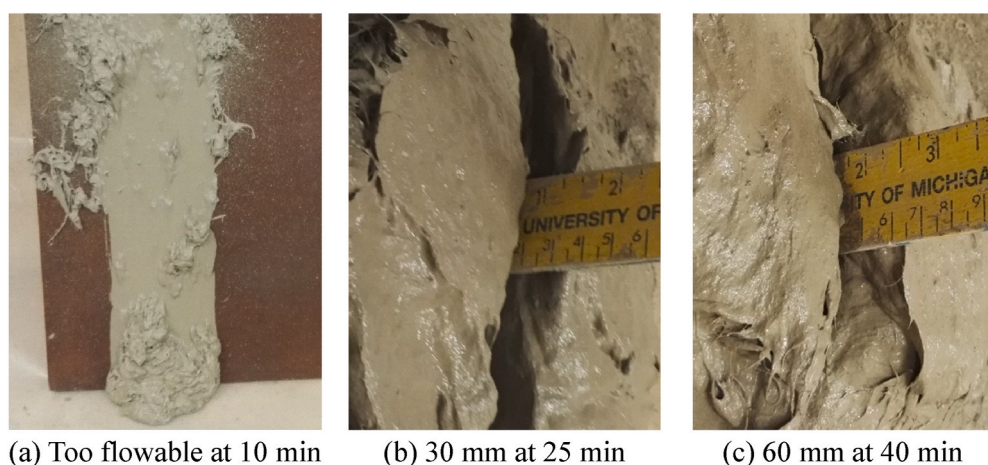


Fig. 8. The build-up thickness of ECC (WR-0.8%) at different rest-time sprayed with the small spray hopper.

atomization and buildability functions. The maximum build-up thickness of the sprayed ECC was 45 mm for vertical spray and 40 mm for overhead spray (Fig. 10). The atomized ECC was sprayed evenly onto the plywood without dripping, sloughing, and rebound. The superior rheological properties contributed by CSA cement and LC3 cement account for the good performance of sprayability. Also, no aggregates (sand, stone) were used for the ECC composition in this study. The lower density of the ECC reduced the defects caused by the negative effects of gravity [8]. Further, the material cost is reduced due to less waste of ECC caused by dripping and rebound that demand an additional 5–8% material cost in typical shotcreting operation.

4.2. Uniaxial tensile performance

Ultra-high ductility contributed by multi-cracks is the unique property of ECC. Fig. 11 (a) illustrates the tensile stress and strain relationship of the sprayed ECC and the cast ECC. Both the first cracking strength and the ultimate tensile strength of sprayed ECC were lower than that of cast ECC. The ultimate tensile strength of the cast ECC (2.8 MPa) decreased to 2.6 MPa due to the spray processing. A 10% reduction of compressive strength was found for sprayed ECC compared with the cast ECC (from 22.1 MPa to 20.0 MPa as listed in Table 2). However, the tensile strain capacity of the sprayed ECC was increased from 4.7% to 5.7% compared to the cast ECC.

The spray process affects the air content of the matrix and the mechanical property of the sprayed ECC. Usually, minimizing the air voids or squeezing out the excess air could mitigate the negative effect of air entrainment by spray process, e.g., the sprayed ECC obtained a comparable strength and ductility to the cast ECC [5] by properly designing the sprayability. However, some studies ignored the atomization quality of the sprayable ECC, resulting in excess air voids in the matrix during the spray process. The macro flaws reduced the matrix strength and affected the fiber dispersion, leading to reduced strength and ductility [40,41]. Approximate 20–50% of the ultimate tensile strength and 20–67% of tensile strain capacity reductions were observed [14,29,40, 41], as summarized in Table 3. Another method is introducing excess air in the original composition and squeezing out the excess air during the spraying process, leading to a more compacted matrix than the cast one [42]. However, controlling the air content in practical engineering is difficult, especially during the spray process, uncontrollable air content leads to the variation of mechanical performance.

In this study, the fresh property of the sprayed ECC was deliberately designed using CSA cement, LC3 cement, and PP fiber. The good atomization quality led to the compact matrix and avoided large voids in the sprayed ECC. Therefore the ultimate tensile strength was only 0.2 MPa lower compared to the cast ECC. The flaws imported by sprayed air promoted the initiation of the cracks, attaining a larger tensile strain

capacity. Fig. 12 illustrates that the sprayed ECC generated more cracks than the cast ECC, improving the ductility of the sprayed ECC. Fig. 11(b) shows that the sprayed ECC presented smaller observed crack width at all strain levels. The relatively large crack width is one of the main challenges for the PP-ECC when compared with PVA-ECC [30]. The average crack width of cast ECC was 75–150 μm , which was comparable to the published results [29,30]; however, significantly larger than that of the PVA-ECC (30–80 μm). The average crack width of the sprayed ECC was only 30 μm at 1% and below 90 μm at 5%. While the average crack width was below 100 μm , the maximum crack width (Fig. 11 (c)) of both cast and sprayed ECC was nearly 3 times the average crack width, consistent with [43]. The tiny crack width was attributed to more cracks initiated at a relatively low-stress level due to the flaw imported by air. Though the mechanical properties of PP fiber are inferior to PVA fiber, the sprayed ECC reinforced with PP fiber had comparable average crack width and superior ductility than the sprayed ECC with PVA fiber, and smaller maximum crack width than that reported for PVA-ECC [43].

4.3. Flexural and bonding performance of ECC-concrete layered composite

The flexural load and deflection response of the ECC-concrete composite is illustrated in Fig. 13. No obvious differences in load capacity were found between the sprayed ECC-concrete and cast ECC-concrete composites. Under plane cross-section assumption per [44], the first crack occurred in the bottom ECC layer at approximately 4 MPa, which was comparable to the commercial polymer repair mortar reported in Refs. [5]. Distinct from conventional mortar, the ECC-concrete sustained a higher load after the first crack due to the pseudo strain-hardening property of ECC. The ultimate flexural strength increased to 5.6 MPa and 5.9 MPa for sprayed and cast ECC-concrete composite, respectively. Similar to uniaxial tensile properties, the sprayed ECC-concrete displayed a slightly lower strength and higher deflection, attributed to the air voids and increased ductility of the sprayed ECC.

The deflection capacity of the layered ECC-concrete was 7.4–8.1 mm (Table 2), which was more than 30 times that of the concrete repaired with commercial polymer mortar [5]. Although the average deflection capacity of the sprayed ECC was comparable to that of the cast ECC, the sprayed specimens showed greater variability, plausibly due to the increased flaw size range induced by air entrainment. Compared to the concrete repair with PVA-ECC [5], the deflection capacity in this study was increased more than two times. A larger deflection capacity is more important than the higher strength capacity, especially for repairing infrastructure such as bridge, tunnel, and pavement, of which the cracks were mainly caused by uneven/imposing deformation other than overload. The high ductility of ECC assures improved deformation capacity, and energy absorption capacity for the ECC repaired system.

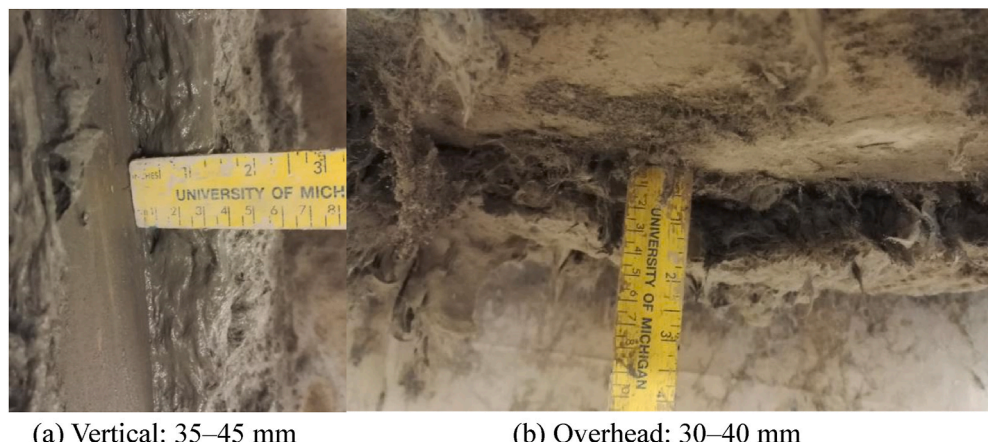


Fig. 10. Spray test using the CARROUSEL® pump.

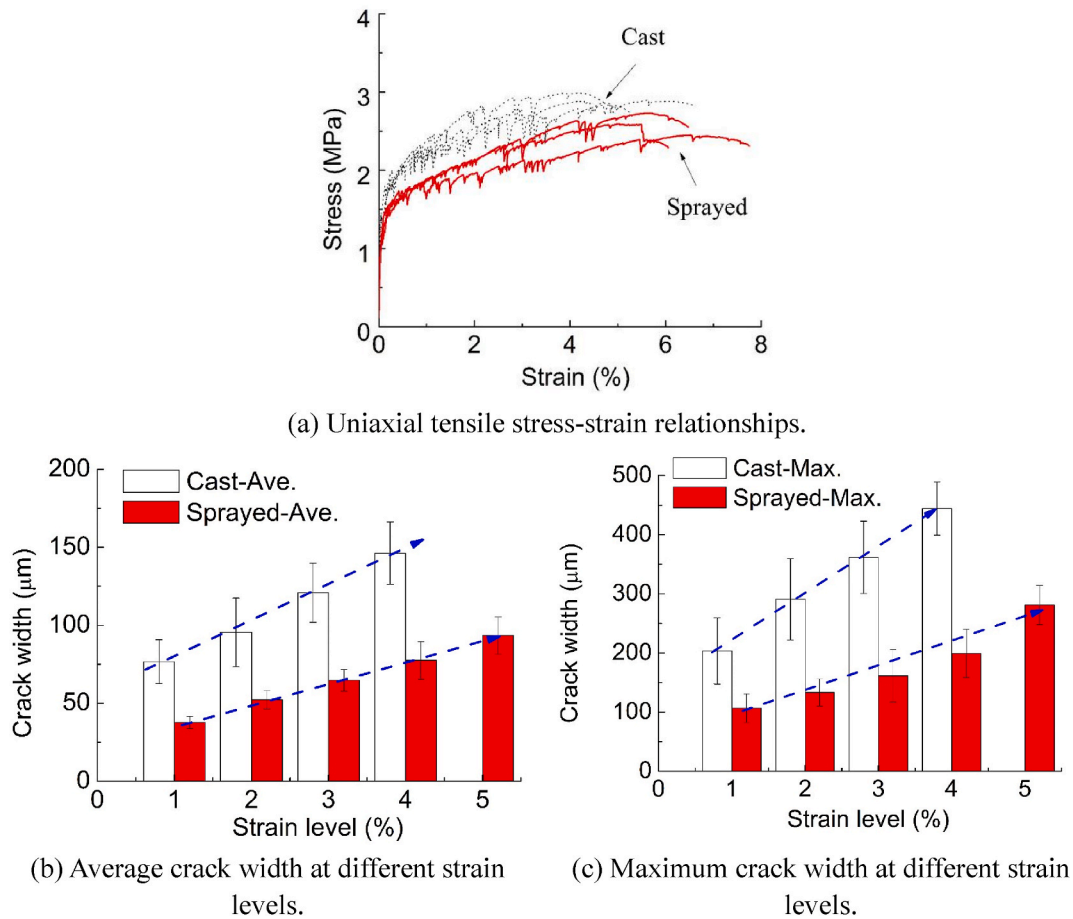


Fig. 11. Tensile performance of the sprayed ECC and cast ECC.

Table 2
Measured mechanical performance of the sprayed and cast ECC.

	f_c (MPa)	f_{split} (MPa)	f_t (MPa)	ϵ_t (%)	F_{bend} (N)	Deflection (mm)
No. of specimens	3	6	3		4	
Cast	22.1 ± 0.5	2.3 ± 0.6	2.8 ± 0.2	4.7 ± 0.9	2812 ± 176	7.4 ± 0.7
Sprayed	20.0 ± 0.7	2.2 ± 0.4	2.6 ± 0.2	5.7 ± 0.8	2695 ± 290	8.1 ± 4.2

Note: f_c , f_{split} , f_t , ϵ_t , and F_{bend} denotes the compressive strength, splitting tensile strength of interfacial bonding, ultimate tensile strength, tensile strain capacity, and flexural load.

Table 3

The comparison of the tensile strength and strain capacity performance in previous researches.

Tensile performance	\downarrow^a	\approx^a	\uparrow^a
Reference	[29]	[14]	[40]
f_t (MPa)	Cast	1.1	3.0
	Spray	0.9	2.2
ϵ_t (%)	Cast	3.0	3.0
	Spray	1.0	2.3

^a The notation \uparrow , \approx , \downarrow represents the tensile performance was increased, comparable, and decreased by the spray process.

Fig. 14 displays the crack patterns of the flexural ECC-concrete composite. As the load increased, the first crack was observed in the ECC layer around the midspan of the composite. During the pseudo



Fig. 12. Crack patterns of the dogbone samples unloaded after the final tested points shown in Fig. 11(a).

strain-hardening stage, more microcracks were generated in the ECC, and the cracks propagated up to the concrete layer. Eventually, a macro crack was formed in the midspan of the concrete layer. As the load continued to increase, the concrete macrocrack propagated along with the interface of ECC and concrete, and more cracks were generated in the bottom ECC layer. The ECC worked as a plastic hinge, redistributing the stress. The crack width of concrete was also restrained, leading to no local failure in the ECC-concrete composite. Further increase in load generated more microcracks in the ECC layer, and the concrete layer also presented multiple cracking properties.

Since no deliberate roughening of the concrete surface was introduced prior to ECC spraying, full bonding between the two materials that could lead to concrete spalling [36] was avoided. Instead, the moderate bond promoted local debonding along the interface at

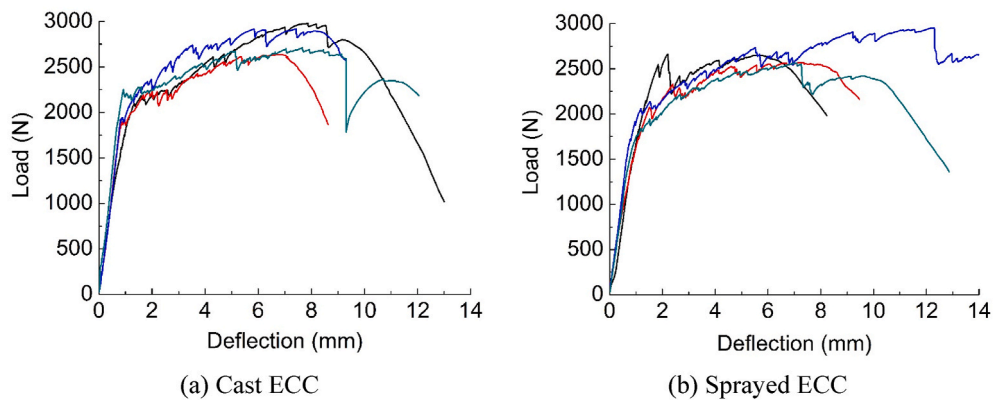


Fig. 13. Flexural load versus deflection relationships of ECC-concrete composite.

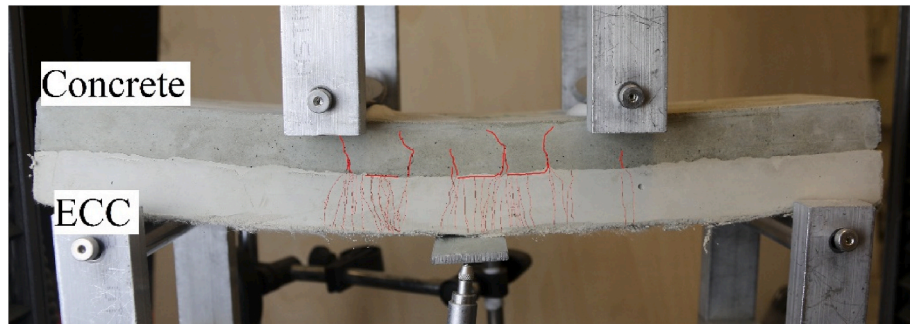


Fig. 14. The crack patterns of the ECC-concrete composite under flexural loading.

midspan (Fig. 14), leading to more microcracks in ECC as loading increased. No delamination failure was found, indicating that the ECC-concrete worked as an integral composite element under flexural load. ECC-concrete composite altered the failure mode from brittle to ductile.

The interfacial bond strength was measured by a split tensile test consistent with [8]. Though the measured strength depends on the interface roughness and specimen geometry [39,45], it is suitable for demonstrating the difference between cast ECC and sprayed ECC under the same testing condition. The bond strength of sprayed and cast ECC was found comparable (Table 2), indicating that the sprayed process had little effect on the interfacial bonding. Meanwhile, a commercial polymer modified mortar [5] expected to have an enhanced bond performance was used as a reference. The bond strength of the polymer-modified mortar was 2.07 MPa, slightly lower than the developed ECC. Xu [8] proved that the interface roughness had a more significant influence on the interfacial shear strength than on the interfacial bond strength. The increased shear resistance due to rough surface impedes the cracks propagating along with the ECC-concrete interface [8], leading to local failure in the concrete layer [5], rather than the multiple cracks as observed in Fig. 14. Meanwhile, a strong bond between the ECC and concrete may lead to reflective cracking and limit the ductility of ECC-concrete composite [36]. Hence, the rough interface was not recommended for the ECC-concrete repair system under flexure. The optimal interface roughness for assuring both bonded and flexural performance requires further studies.

5. Conclusions

A sprayable ECC was developed using LC3 cement, CSA cement, and PP fiber with characteristics of low carbon, low shrinkage, and low cost for infrastructure repair. The fresh properties were deliberately designed suitable for spraying while maintaining ultra-high tensile ductility. The following conclusions can be drawn:

- Flow table test is found to be a simple and practical method for designing the rheology of sprayable ECC. The maximum deformability index of 2.5 is proposed for thickness build-up without dripping, while the minimum deformability index of 1.8 is recommended for good atomization quality of ECC at the spray nozzle. The spray air pressure should not exceed 500 kPa for the PP-ECC to maintain cohesiveness between the hydrophobic PP fiber and the matrix during spray operation. The deformability range determined assures the attainment of desired fresh and hardened performance of the sprayable ECC.
- The desired two-stage rheology for sprayability is found to be attainable through tailoring the amount of CSA cement and water reducer. As a result, a build-up thickness of 45 mm for vertical spraying and 30 mm for overhead spraying was achievable at 20–30 min rest time. The maximum build-up thickness could reach 78 mm for vertical spraying at 50 min rest time.
- Good material atomization at the spray nozzle is found necessary for minimization of large flaws caused by air entrainment in the sprayed ECC. As a result, minimal differences in compressive and tensile strength were found between spraying and casting processes.
- Through deliberate design of ECC matrix and atomization quality, the sprayable PP-ECC developed in this study attained a remarkable tensile strain capacity of 5.7%, significantly larger than that previously reported for sprayed ECC reinforced with PVA fiber. The crack width of the sprayed PP-ECC during strain-hardening was 30–90 μm , comparable to that of PVA-ECC.
- For the ECC-concrete composite, fracture localization in the concrete layer was found to be suppressed by the strain-hardening ECC. The ECC-concrete composite worked as an integral structure without delamination, revealing multiple cracking and strain hardening effects with a ductile failure mode. This modified behavior suggested a highly durable repaired system using sprayable ECC.

Declaration of competing interest

The authors declare that they have no known competing financial interests or personal relationships that could have appeared to influence the work reported in this paper.

Acknowledgments

This research is partially supported by the Center for Low Carbon Built Environment (CLCBE) at the University of Michigan. Materials supplies from BORAL RESOURCES (fly ash), GCP Applied Technologies (water reducer), CTS Cement Manufacturing Corp. (CSA cement), Omya (limestone), and Sika (metakaolin) are gratefully acknowledged.

Appendix A. Supplementary data

Supplementary data to this article can be found online at <https://doi.org/10.1016/j.cemconcomp.2020.103868>.

References

- [1] V.C. Li, Engineered Cementitious Composites (ECC): Bendable Concrete for Sustainable and Resilient Infrastructure, Springer, 2019.
- [2] N. Roghanian, N. Banthia, Development of a sustainable coating and repair material to prevent bio-corrosion in concrete sewer and waste-water pipes, *Cement Concr. Compos.* 100 (2019) 99–107.
- [3] E.S. Bernard, Age-dependent changes in post-crack performance of fibre reinforced shotcrete linings, *Tunn. Undergr. Space Technol.* 49 (2015) 241–248.
- [4] Y.Y. Kim, H. Kong, V.C. Li, Design of engineered cementitious composite suitable for wet-mixture shotcreting, *ACI Mater. J.* 100 (2003) 511–518.
- [5] Y.Y. Kim, G. Fischer, Y.M. Lim, V.C. Li, Mechanical performance of sprayed engineered cementitious composite using wet-mix shotcreting process for repair applications, *ACI Mater. J.* 101 (2004) 42–49.
- [6] V.C. Li, G. Fischer, M. Lepech, Shotcreting with ECC, Spritzbeton-Tagung, Austria, 2009.
- [7] Y. Lin, D. Biggs, L. Wotherspoon, J.M. Ingham, In-plane strengthening of unreinforced concrete masonry wallettes using ECC shotcrete, *J. Struct. Eng.* 140 (2014), 04014081.
- [8] S. Xu, F. Mu, J. Wang, W. Li, Experimental study on the interfacial bonding behaviors between sprayed UHTCC and concrete substrate, *Construct. Build. Mater.* 195 (2019) 638–649.
- [9] S. Müller, V. Mechtricherine, Use of Strain-Hardening Cement-Based Composites (SHCC) for Retrofitting, International Conference on Concrete Repair, Rehabilitation and Retrofitting (ICCR 2018), EDP Sciences, 2018, 09006.
- [10] J.S. Davidson, J. Kang, T.C. Grimes, J. Farrell, U.K. Vaidya, B. Pillay, B. Thattaiaparhasarat, PVA fiber reinforced shotcrete for rehabilitation and preventative maintenance of aging culverts, in: U.D.O.C. Auburn, C.A.H.D. Shelby, E.C. Blascrete (Eds.), University Of Alabama At Birmingham. Dept. Of Civil, 2009.
- [11] Y.C. Díaz, S.S. Berriel, U. Heierli, A.R. Favier, I.R.S. Machado, K.L. Scrivener, J.F. Hernández, G. Habert, Limestone calcined clay cement as a low-carbon solution to meet expanding cement demand in emerging economies, *Development Engineering* 2 (2017) 82–91.
- [12] S. Gao, Z. Wang, W. Wang, H. Qiu, Effect of shrinkage-reducing admixture and expansive agent on mechanical properties and drying shrinkage of Engineered Cementitious Composite (ECC), *Construct. Build. Mater.* 179 (2018) 172–185.
- [13] J. Zhang, C. Gong, Z. Guo, M. Zhang, Engineered cementitious composite with characteristic of low drying shrinkage, *Cement Concr. Res.* 39 (2009) 303–312.
- [14] G.P. van Zijl, L. de Beer, Sprayed strain-hardening cement-based composite overlay for shear strengthening of unreinforced load-bearing masonry, *Adv. Struct. Eng.* 22 (2018) 1121–1135.
- [15] H. Zhu, Y. Hu, Q. Li, R. Ma, Restrained cracking failure behavior of concrete due to temperature and shrinkage, *Construct. Build. Mater.* 244 (2020) 118318.
- [16] K. Scrivener, F. Martirena, S. Bishnoi, S. Maity, Calcined clay limestone cements (LC3), *Cement Concr. Res.* 114 (2018) 49–56.
- [17] K.L. Scrivener, Options for the future of cement, *Indian Concr. J.* 88 (2014) 11–21.
- [18] S.S. Berriel, A. Favier, E.R. Domínguez, I.R.S. Machado, U. Heierli, K. Scrivener, F. Martirena, Hernández, G. Habertd, Assessing the environmental and economic potential of limestone calcined clay cement in Cuba, *J. Clean. Prod.* 124 (2016) 361–369.
- [19] H. Zhu, D. Zhang, T. Wang, H. Wu, V.C. Li, Mechanical and self-healing behavior of low carbon engineered cementitious composites reinforced with PP-fibers, *Construct. Build. Mater.* 259C (2020) 119805.
- [20] J. Yu, H. Wu, C.K.Y. Leung, Feasibility of using ultrahigh-volume limestone-calcined clay blend to develop sustainable medium-strength Engineered Cementitious Composites (ECC), *J. Clean. Prod.* (2020) 121343.
- [21] K. Vance, A. Kumar, G. Sant, N. Neithalath, The rheological properties of ternary binders containing Portland cement, limestone, and metakaolin or fly ash, *Cement Concr. Res.* 52 (2013) 196–207.
- [22] F. Nazário Santos, S. Raquel Gomes De Sousa, A. José Faria Bombard, S. Lopes Vieira, Rheological study of cement paste with metakaolin and/or limestone filler using Mixture Design of Experiments, *Construct. Build. Mater.* 143 (2017) 92–103.
- [23] I.A. Chen, C.W. Hargis, M.C.G. Juenger, Understanding expansion in calcium sulfoaluminate–belite cements, *Cement Concr. Res.* 42 (2012) 51–60.
- [24] W. Choi, H. Yun, Effect of expansive admixtures on the shrinkage and mechanical properties of high-performance fiber-reinforced cement composites, *Sci. World J.* (2013) 2013.
- [25] J. Bizzozero, C. Gosselin, K.L. Scrivener, Expansion mechanisms in calcium aluminate and sulfoaluminate systems with calcium sulfate, *Cement Concr. Res.* 56 (2014) 190–202.
- [26] K. Yu, Y. Ding, J. Liu, Y. Bai, Energy dissipation characteristics of all-grade polyethylene fiber-reinforced engineered cementitious composites (PE-ECC), *Cement Concr. Compos.* 106 (2020) 103459.
- [27] K. Yu, Y. Wang, J. Yu, S. Xu, A strain-hardening cementitious composites with the tensile capacity up to 8%, *Construct. Build. Mater.* 137 (2017) 410–419.
- [28] K. Yu, Z. Lu, J. Dai, S.P. Shah, Direct tensile properties and stress-strain model of UHP-ECC, *J. Mater. Civ. Eng.* 32 (2020), 04019334.
- [29] Q. Zhang, V.C. Li, Development of durable spray-applied fire-resistive engineered cementitious composites (SFR-ECC), *Cement Concr. Compos.* 60 (2015) 10–16.
- [30] B. Felekoglu, K. Tosun-Felekoglu, R. Ranade, Q. Zhang, V.C. Li, Influence of matrix flowability, fiber mixing procedure, and curing conditions on the mechanical performance of HTPP-ECC, *Compos. B Eng.* 60 (2014) 359–370.
- [31] M. Li, V.C. Li, Rheology, fiber dispersion, and robust properties of Engineered Cementitious Composites, *Mater. Struct.* 46 (2013) 405–420.
- [32] ASTM C1437-15, Standard Test Method for Flow of Hydraulic Cement Mortar, ASTM International, West Conshohocken, PA, 2015.
- [33] E. Secrieru, V. Mechtcherine, C. Schröfl, D. Borin, Rheological characterisation and prediction of pumpability of strain-hardening cement-based-composites (SHCC) with and without addition of superabsorbent polymers (SAP) at various temperatures, *Construct. Build. Mater.* 112 (2016) 581–594.
- [34] J.S. Kim, S.H. Kwon, K.P. Jang, M.S. Choi, Concrete pumping prediction considering different measurement of the rheological properties, *Construct. Build. Mater.* 171 (2018) 493–503.
- [35] E. Yang, M. Sahmaran, Y. Yang, V.C. Li, Rheological control in production of engineered cementitious composites, *ACI Mater. J.* 106 (2009) 357.
- [36] G.P.A.G. van Zijl, D.J.A. de Jager, Improved ductility of SHCC retrofitted unreinforced load bearing masonry via a strip-debonded approach, *Journal of Building Engineering* 24 (2019) 100722.
- [37] ASTM C109-Standard Test Method for Compressive Strength of Hydraulic Cement Mortars, ASTM International, West Conshohocken, PA, 2020.
- [38] ASTM C496/C496M-17, Standard Test Method for Splitting Tensile Strength of Cylindrical Concrete Specimens, ASTM International, West Conshohocken, PA, 2017.
- [39] S. Carmona, A. Aguado, New model for the indirect determination of the tensile stress-strain curve of concrete by means of the Brazilian test, *Mater. Struct.* 45 (2012) 1473–1485.
- [40] S. Xu, B. Zhou, Q. Li, Y. Wu, Mechanical performance of spareable ultra high toughness cementitious composites, *J. Hydraul. Eng.* 46 (2015) 619–625.
- [41] J. Kim, J. Kim, G.J. Ha, Y.Y. Kim, Rheological control of cement paste for applying prepackaged ECCs (Engineered Cementitious Composites) to self-consolidating and shotcreting processes, *KSCE J. Civ. Eng.* 14 (2010) 743–751.
- [42] T. Kanda, T. Saito, N. Sakata, M. Hiraishi, Tensile and anti-spalling properties of direct sprayed ECC, *J. Adv. Concr. Technol.* 1 (2003) 269–282.
- [43] G.P. van Zijl, V. Slowik, R.D. Toledo Filho, F.H. Wittmann, H. Mihashi, Comparative testing of crack formation in strain-hardening cement-based composites (SHCC), *Mater. Struct.* 49 (2016) 1175–1189.
- [44] ASTM C1161-18, Standard Test Method for Flexural Strength of Advanced Ceramics at Ambient Temperature, ASTM International, West Conshohocken, PA, 2018.
- [45] Q. Zhang, V.C. Li, Adhesive bonding of fire-resistive engineered cementitious composites (ECC) to steel, *Construct. Build. Mater.* 64 (2014) 431–439.